\$ SUPER

Contents lists available at ScienceDirect

# Water Research

journal homepage: www.elsevier.com/locate/watres





# Stormwater biofilter response to high nitrogen loading under transient flow conditions: Ammonium and nitrate fates, and nitrous oxide emissions

Marina Feraud <sup>a</sup>, Sean P. Ahearn <sup>b</sup>, Emily A. Parker <sup>c</sup>, Sumant Avasarala <sup>d</sup>, Megyn B. Rugh <sup>e</sup>, Wei-Cheng Hung <sup>e</sup>, Dong Li <sup>a</sup>, Laurie C. Van De Werfhorst <sup>a</sup>, Timnit Kefela <sup>a</sup>, Azadeh Hemati <sup>c</sup>, Andrew S. Mehring <sup>f</sup>, Yiping Cao <sup>g,h</sup>, Jennifer A. Jay <sup>e</sup>, Haizhou Liu <sup>i</sup>, Stanley B. Grant <sup>c,j</sup>, Patricia A. Holden <sup>a,\*</sup>

- a Bren School of Environmental Science and Management, University of California, Santa Barbara, Santa Barbara, CA, United States
- b Research & Development Beta Analytic, Inc., Miami, FL, United States
- c The Charles E. Via, Jr. Department of Civil and Environmental Engineering, Occoquan Watershed Monitoring Laboratory, Virginia Tech, Manassas, VA, United States
- <sup>d</sup> Department of Earth and Planetary Sciences, University of Tennessee, Knoxville, TN, United States
- e Department of Civil and Environmental Engineering, UCLA, Los Angeles, CA 90095, United States
- f Department of Biology, University of Louisville, Louisville, KY, United States
- <sup>g</sup> Source Molecular Corporation, Miami Lakes, FL, United States
- <sup>h</sup> Santa Ana Water Quality Control Board, Riverside, CA, United States
- i Department of Chemical and Environmental Engineering, UC Riverside, Riverside, CA, United States
- <sup>j</sup> Center for Coastal Studies, Virginia Tech, Blacksburg, VA, United States

### ABSTRACT

Nitrogen (N) in urban runoff is often treated with green infrastructure including biofilters. However, N fates across biofilters are insufficiently understood because prior studies emphasize low N loading under laboratory conditions, or use "steady-state" flow regimes over short time scales. Here, we tested field scale biofilter N fates during simulated storms delivering realistic transient flows with high N loading. Biofilter outflow ammonium (NH $\ddagger$ -N) was 60.7 to 92.3% lower than that of the inflow. Yet the characteristic times for nitrification (days to weeks) and denitrification (days) relative to N residence times (7 to 30 h) suggested low N transformation across the biofilters. Still, across 7 successive storms, total outflow nitrate (NO $_3$ -N) greatly exceeded (3100 to 3900%) inflow nitrate, a result only explainable by biofilter soil N nitrification occurring between storms. Archaeal, and bacterial *amo*A gene copies (2.1  $\times$  10<sup>5</sup> to 1.2  $\times$  10<sup>6</sup> gc g soil $^{-1}$ ), nitrifier presence by16S rRNA gene sequencing, and outflow  $\delta^{18}$ O-NO $_3$  values (-3.0 to 17.1 %) reinforced that nitrification was occurring. A ratio of  $\delta^{18}$ O-NO $_3$  to  $\delta^{15}$ N-NO $_3$  of 1.83 for soil eluates indicated additional processes: N assimilation, and N mineralization. Denitrification potential was suggested by enzyme activities and soil denitrifying gene copies (nirK + nirS:  $3.0 \times 10^6$  to  $1.8 \times 10^7$ ; nosZ:  $5.0 \times 10^5$  to  $2.2 \times 10^6$  gc g soil $^{-1}$ ). However, nitrous oxide (N<sub>2</sub>O-N) emissions (13.5 to 84.3 µg N m  $^{-2}$  h  $^{-1}$ ) and N<sub>2</sub>O export (0.014 g N) were low, and soil nitrification enzyme activities (0.45 to 1.63 mg N kg soil $^{-1}$ day $^{-1}$ ). Taken together, chemical, bacterial, and isotopic metrics evidenced that storm inflow NH $_4$ sorbs and, along with mineralized osil N, nitrifies during biofilter dry-down; little denitrification and associated N<sub>2</sub>O emissions ensue, and thus subsequent storms export copious NO $_3$ -N. As such, pulsed pass-through biofilters require redesign to promote plant ass

# 1. Introduction

Anthropogenic inputs of reactive nitrogen (N) to the environment exceed sustainable planetary boundaries (Steffen et al. 2015), indicating a critical need for effective management practices. Excess N loading into coastal waters, for example from untreated stormwater runoff (Walsh et al., 2004), causes hypoxia which disrupts ecosystems and fisheries (Schlesinger 2009). To reduce impacts from runoff, green stormwater infrastructure (GSI) such as biofilters capture flow to remove suspended

solids, metals, fecal bacteria (Davis et al., 2001; Bratieres et al., 2008; Li et al., 2021), and pathogens and antibiotic resistant bacteria (Rugh et al., 2022). Over 70% of biofilter inflow N may be removed (Davis et al., 2001; Bratieres et al., 2008), largely via ammonium (NH<sub>4</sub><sup>†</sup>) sorbing to biofilter soils, NH<sub>4</sub><sup>†</sup> nitrifying to nitrate (NO<sub>3</sub><sup>-</sup>), and NO<sub>3</sub><sup>-</sup> denitrifying to gaseous N forms (N<sub>2</sub>, NO, and N<sub>2</sub>O) (Payne et al., 2014a). However, denitrification depends on biofilter design factors including soils and plants (Bratieres et al., 2008; Read et al., 2010), and including a saturated zone amended with organic carbon (Zinger et al., 2013; Payne

E-mail address: holden@bren.ucsb.edu (P.A. Holden).

<sup>\*</sup> Corresponding author.

et al., 2014b). Without significant denitrification,  $NO_3^-$  leaches as a mobile pollutant (Davis et al., 2001; Bratieres et al., 2008). Therefore, understanding  $NO_3^-$ -N export in field-scale biofilters under realistic operating conditions is needed.

Overall, N entering biofilters may sorb to soils, assimilate into plants, transform abiotically, or microbially immobilize or transform (Payne et al., 2014a). Prior studies provide insights. For example, in a field scale biofilter, particulate organic N (PON) dissolved to organic N (DON) which mineralized to NH<sub>4</sub>; NH<sub>4</sub> nitrified to NO<sub>3</sub>, and plants assimilated NH<sub>4</sub><sup>+</sup> and NO<sub>3</sub><sup>-</sup> (Li and Davis 2014). In biofilter mesocosms, inflow N minimally denitrified but rapidly assimilated into plants (Payne et al., 2014b). Biofilter mesocosms may remove only 1.4% of inflow NO<sub>3</sub> (Burgis et al., 2020). The preceding studies, however, are either small scale or hydrologically unrealistic, and field scale hydrologic regimes of transient flows are infrequently studied (Davis 2007, Brown and Hunt 2011, Burgis et al., 2020). Under realistic transient flows, soils are intermittently saturated, resulting in drier soils and unfavorable conditions for denitrification. This contrasts with steady flow conditions that promote saturation and thus denitrification and permanent N removal (Zinger et al., 2013; Payne et al., 2014a). Field studies evaluating individual storms (Hunt et al., 2006; Hatt et al., 2009; Brown and Hunt 2011) do not address drying and rewetting and thus how the antecedent dry period influences NO3 formation and N fates during successive storms. N exported during one storm depends on prior storm characteristics and antecedent conditions (Brown et al., 2013). Further, when loading biofilters with low-N runoff during successive storms, NO<sub>3</sub> accumulates during dry periods (Li and Davis 2014). However, NO3-N may derive from influent N, and thus increase as N loading to biofilters increases (Brown et al., 2013). Taken together, how biofilters process N from realistic, highly polluted transient flows—as would occur during the large first-flush of storms —is weakly understood. Further, how N processing between storms affects biofilter N treatment variation, is unknown. A better understanding of processes controlling aqueous and gaseous N emissions under realistic conditions is needed to improve biofilter operations and designs to enhance N removal via denitrification.

For full scale biofilters conveying transient flow runoff from successive simulated storms—including when runoff was highly N-contaminated such that N fates were measurable—this study evaluated: (1)  $\rm NH_4^+$  and  $\rm NO_3^-$  fates, and  $\rm N_2O$  fluxes; (2)  $\rm NO_3^-$  isotopic evidence of predominant N transformations within and between storms; (3) potential microbial processes by quantifying genes encoding bacterial 16S rRNA, nitrification, and denitrification; (4) mass balance-based evidence of  $in \, situ \, NH_4^+$ , and  $\rm NO_3^-$  generation (via mineralization and nitrification, respectively). The findings point to nitrification predominating between storms, regardless of how inflow N was processed during a storm. The results suggest future considerations for mitigating biofilter N emissions.

# 2. Methods

# 2.1. Experimental design and hydrology

Experiments were conducted on two full-scale biofilters (control biofilter "C2" and test biofilter "C4") at the Orange County Public Works (OCPW) Glassell campus (Orange, CA) where the summers are warm and dry, and winters are mild. Annual precipitation is 37 cm, occurring mostly during winter (December – March) (National Oceanographic and Atmospheric Administration, 2021). The biofilters were 2.4 m long, 1.5 m wide, and 1.8 m deep (Fig. S1 and Table S1) and were planted with Carex spissa. Soil (depth 0.6 m) consisted of a sandy loam with 85–88% sand, 8 - 12% fines, and 3 - 5% organic matter. The biofilters are contiguous, both constructed in 2016, and identically designed. The biofilters were dosed with either unspiked, or sewage-spiked (50% by volume), stormwater runoff. Soils, and aqueous and gaseous emissions were studied.

Transient flows were imposed through the biofilters following a

hydrograph constructed from storms observed in Orange County and adjusted to represent an 85th percentile storm (Fig. S2). Time series of infiltration, gravitational discharge, and soil saturation were obtained by solving the one-dimensional Richards equation (Hydrus 1D, Version 4.17.0140, PC-Progress), using measured inflows and potential evapotranspiration estimates, as described previously (Parker et al., 2021).

Runoff or mixed inflows were transiently dosed. The runoff—sourced from an adjacent parking lot and a treatment wetland—was collected and stored (less than 6 months) in an underground cistern. The runoff was partially treated via a hydrodynamic separator that removed particulate matter and trash. Bypass flows during large storms had been directed to a treatment wetland (Modular Wetland, Bioclean, Oceanside, CA). A mixed inflow was prepared by combining 750 L raw sewage from the Orange County Sanitation District wastewater treatment plant with 750 L stormwater runoff. Further details are published (Parker et al., 2021). This relatively high N loading simulated an extreme event and provided experimental resolution. The biofilters were conditioned with runoff (storms S1–2), after which biofilter C2 was sacrificed to collect baseline soil cores. Biofilter C4 then received 1:1 mixed inflow (storm S3) and was subsequently flushed with runoff (storms S4–7). Following flushing, endpoint soil cores were collected (Fig. S3).

# 2.2. Water and soil sampling

Runoff or mixed inflow were sampled from the inflow tank 2 to 4 times per storm, while biofilter outflow was sampled every 10 min. For storms S1 and S2, ten outflow samples were collected from the shared biofilter underdrain (Fig. S1) using a peristaltic pump (flow rate 0.23 L/min). For storms S3–7, 21 to 28 outflow samples were collected per storm, from a sump located at the end of a manifold through which biofilter C4 outflow drained. Biofilter outflow was pumped (Model 98 Sump Pump, Zoeller Pump Company, Louisville, KY) from the sump into a continuously overflowing 5 L bucket, which was sub-sampled by a peristaltic pump (20 mL/min) (BioLogic LP, Bio-Rad, Hercules, CA) and fractionated every 5 min until outflow ceased. Water samples were filtered through a 0.45  $\mu$ m PES syringe filter (Whatman Uniflo, GE Healthcare, Chicago, IL), collected into 50 mL conical tubes and refrigerated (4 °C) until NH $_4^+$  and NO $_3^-$  analysis (within two weeks).

Soil samples at depths of 0 to 10 cm, 10 to 20 cm, 30 to 40 cm, and 50 to 60 cm were collected via coring; soil cores were sieved through a brass 2-mm mesh (No. 10) (Advantage Manufacturing, Inc., New Berlin, WI), subsampled, transported, and stored (4 °C, except for subsamples for DNA extraction, NH $_4^+$ , and NO $_3^-$ : -20 °C) until analysis (two days, except for NH $_4^+$ , NO $_3^-$ , total carbon (TC), total nitrogen (TN), cation exchange capacity (CEC), and particle size analysis, which occurred within six weeks), and soil eluates were generated onsite (Supplemental Methods).

# 2.3. Biofilter soil, aqueous inflow and outflow, and soil eluate analyses

Analysis of soil gravimetric moisture content, organic matter via loss on ignition (SOM-LOI), pH, bulk density, and concentrations of  $NH_{\tau}^{+}, NO_{3}^{-},$  and dissolved organic carbon (DOC) followed established approaches (Supplemental Methods). A 500 g soil subsample was shipped to the UC Davis Analytical Lab (https://anlab.ucdavis.edu/) for TC, TN, CEC, and particle size analyses. Soil microbial biomass was assessed by the substrate induced respiration (SIR) method. Nitrifying and denitrifying enzyme activities (NEA and DEA) were assessed via the chlorate inhibition, and acetylene reduction, methods, respectively (Supplemental Methods).

Aqueous NH $_4^+$  and NO $_3^-$  concentrations were measured following EPA Method 350.1 (U.S. EPA 1993), and EPA Method 300.0 (U.S. EPA 1997), respectively (Supplemental Methods). Mass flow rates and percent relative mass removal were computed (Supplemental Methods, eqs. S1, S2, S3). Aqueous samples and soil eluates were analyzed for nitrate isotopic ratios ( $\delta^{15}$ N-NO $_3^-$ and  $\delta^{18}$ O-NO $_3^-$ ) (Section 2.5).

### 2.4. CO<sub>2</sub>-C, CH<sub>4</sub>-C and N<sub>2</sub>O-N fluxes

Surface soil  $CO_2$ ,  $CH_4$ , and  $N_2O$  emissions in C4 (test biofilter) and associated fluxes were assessed using the closed chamber method (Supplemental Methods, eqs. S4, S5 and S6). Calculated  $CO_2$ -C fluxes ( $\mu g/m^2$  h) were divided by the biofilter soil depth to compute C mineralization rates ( $C_{min}$ ,  $\mu g$  C/ $m^3$  h), while CH<sub>4</sub>-C fluxes were used to indicate biofilter anoxia.

Daily  $N_2O$ -N fluxes ( $\mu g/m^2 h$ ) for storms S3–7 were used to compute  $N_2O$ -N mass emissions ( $\mu g$  N) (sum of  $N_2O$ -N mass emissions for storms S3–7). Daily  $N_2O$ -N fluxes were averaged from three daily measurements per day (Table S4). One average daily flux was determined for storm S3, storms S4–5, and storms S6–7. Daily  $N_2O$ -N mass emissions were the product of the average daily flux ( $\mu g$  N/m $^2$  h), the biofilter surface area ( $m^2$ ) and time (24 h).

# 2.5. Dual nitrate isotopic ratio analyses

Stable  $NO_3^-$  isotopic ratios ( $\delta^{15}N\text{-}NO_3^-$  and  $\delta^{18}O\text{-}NO_3^-$ ) were measured in biofilter C4 for storms S3–7 inflows and outflows, and for eluates from endpoint soil cores. Sample aliquots (10 to 40 mL) were filtered through 0.2  $\mu$ m Isopore polycarbonate filters (Millipore Sigma, Burlington, MA) into acidified 40 mL amber vials.  $NO_3^-$  was measured (EPA Method 353.2) (U.S. EPA 1993) using an AQ300 Discrete Analyzer (Seal Analytical, Inc., Mequon, WI). Samples with greater than 0.08 mg N/L were analyzed on a GasBench II system Spectrometer fitted with a denitrification kit and a Delta V Isotope Ratio Mass Spectrometer (Thermo Fisher Scientific, Waltham, MA) (Supplemental Methods).

# 2.6. Soil DNA extraction, qPCR, and 16S rRNA gene sequencing

Soil DNA was extracted in duplicate using the DNeasy PowerSoil Kit (Qiagen, Hilden, Germany). Extracted DNA was pooled, quantified (Quant-iT dsDNA Broad-Range Assay Kit, Invitrogen Co., Waltham, MA), and archived (—20 °C) until analysis. Genes encoding bacterial 16S rRNA, and nitrifying (archaeal and bacterial *amo*A) and denitrifying (*nir*K, *nir*S, *nos*Z) genes, were evaluated via quantitative polymerase chain reaction (qPCR) (Supplemental Materials). 16S rRNA gene sequencing was previously performed (Li et al., 2021), and sequencing data were deposited in NCBI SRA with BioProject ID PRJNA723423 (Li et al., 2021) but consulted here to assess relative abundances of taxa signatory of N processes.

# 2.7. Transport timescales, biological reaction rates, and N species mass balances

Transport times were measured as the stored water age, i.e. the age of the water in the control volume surrounding biofilter soil, obtained from the previously developed residence time distribution for stored water (See Section 2.3 in Parker et al., 2021). N mineralization rates ( $N_{min}$ ,  $\mu g$  N/  $m^3 h$ ) were estimated by assuming a proportionality to organic C mineralization rates ( $C_{min}$ ,  $\mu g$  C/ $m^3 h$ ; eq. S10, Supplemental Methods); characteristic times for N mineralization ( $\tau_{min}$ , h) were calculated from the product of organic N and bulk density divided by  $N_{min}$  (eq. S11, Supplemental Methods). Instead of directly measuring nitrification or denitrification, a range of published *in situ* reaction rates for biofilters were applied (Chen et al., 2019; Wang et al., 2020).

Mass balances for  $NH_4^+$ -N and  $NO_3^-$ -N were calculated for storms S3–7, considering aqueous mass inflows (eq. S1) and outflows (eq. S2), and changes in biofilter soil  $NH_4^+$ -N and  $NO_3^-$ -N masses from initial (before storm S3) to final (after storm S7) conditions-(Supplemental Methods, eqs. S12–13).  $N_2$ O-N emissions, were the sum of daily average  $N_2$ O-N mass emissions for storms S3–7 (Section 2.4, Supplemental Methods, eq. S14).  $N_2$  emissions were not measured owing to the high ambient atmospheric  $N_2$ ; NO emissions were not assessed.

### 2.8. Data analysis

One-way analysis of variance (Kruskal-Wallis) and post-hoc Dunn's tests were used to assess differences across storms for analyte concentrations, mass flow rates,  $N_2O$  emissions, and outflow  $\delta^{15} N\text{-NO}_3^-$  and  $\delta^{18} O\text{-NO}_3^-$ . Pearson product-moment correlations were used to assess the relationships between normally distributed variables including soil saturation, antecedent dry period, and gas fluxes (CO2, CH4, N2O). Spearman rank-order correlations and linear regression were used to assess the relationships between soil characteristics and bacterial parameters. Relative abundances of assigned genera based on 16S rRNA sequencing were calculated by dividing the published number of assigned sequences by the total number of sequences (Li et al., 2021). Statistical analyses were performed with R (version 4.0.1) at a significance level of  $\alpha=0.05$ .

### 3. Results and discussion

# 3.1. Biofilter soil properties in control and test biofilters

Soil properties indicated environmental conditions and changes imposed on test biofilter C4 by the high loading storm (S3) and flushing storms (S4-7). Soil pH was neutral to alkaline (7.5 to 7.7). Gravimetric moisture content ranged from 14.7 to 17.7% in control biofilter C2, and 14.3 to 24.9% in C4, and increased with depth in C4 (Table S2). Soil organic matter (SOM) ranged from 1.71 to 4.19% in C2, and from 2.92 to 3.18% in C4 (Table S2). Imposing additional storms on C4 may have changed SOM distribution relative to C2, such that leaching of dissolved organic fractions decreased surface soil SOM and increased deep soil SOM. Similarly, the higher soil DOC in C2 (14.07 to 17.1%) relative to C4 (7.39 to 11.1%) suggested that DOC was leached by storm inflow (Table S2). Similar trends were observed for TC, except in the bottom soil layer; soil TN appeared uniform with depth. Molar C:N ratios were similar, except near the surface (higher in C2) and at depth (higher in C4) (Table S2). These differences could owe to higher C losses in biofilter C4 from microbial processing and DOC leaching, and higher N loading from storm S3 sewage inputs. Higher N loading to C4 was evidenced by higher NH<sub>4</sub><sup>+</sup>-N and NO<sub>3</sub><sup>-</sup>-N surface soil concentrations relative to C2 (Table S2). The storm inputs did not alter CEC or soil texture, and the percentages of sand, silt and clay were uniform with depth (Table S2). In contrast, microbial biomass (by SIR) decreased with depth, with means ranging from 0.74 to 7.56 mg C/kg dry soil/day. SIR correlated with SOM (Spearman's  $\rho = 0.71$ , p = 0.05), TC ( $\rho = 0.83$ , p = 0.01), and TN (Spearman's  $\rho = 0.72, p = 0.04$ ).

Overall, biofilter soil properties indicated that N processing decreased with soil depth, since surface soil microbial biomass and nutrients were relatively high. The constant CEC and soil texture suggested a uniform capacity to sorb positively charged chemical species such as NUT.

# 3.2. Biofilter infiltration, discharge, and soil saturation

Biofilter hydrology was assessed to infer the timescales over which soils were saturated, and thus likely to support denitrification. Infiltration rates during storms S1–7 ranged from 0 to 19.4 L/min, while discharge ranged from 0 to 16.2 L/min (Fig. S5). Soil saturation ranged from 0.22 to 1, with full saturation reached (for over 43 to 90 min) during dosing, and rapidly declining after infiltration ceased. With consecutive storms and associated soil water retention as dosing progressed through storm S7, denitrification could have become important (Fig. S5).

# 3.3. $NH_4^+$ -N and $NO_3^-$ -N concentrations, mass flow rates, and relative mass removal

Inflow and outflow NH<sub>4</sub><sup>+</sup>-N and NO<sub>3</sub><sup>-</sup>-N concentrations and mass flow

rates were assessed to infer N fates, and to compute relative percent mass N removals.  $NH_4^+$  retention or removal was calculated within one storm, since retained  $NH_4^+$  could be nitrified between storms and leached as  $NO_3^-$  with subsequent storms.

Outflow NH<sub>4</sub><sup>+</sup>-N concentrations in test biofilter C4 ranged from 0.1 to 2.1 mg/L, which were lower than inflow concentrations (ranging from 0.6 to 15.6 mg/L; Fig. 1a), likely due to adsorption and assimilation in biofilter soil (Payne et al., 2014a). NH<sub>4</sub>-N outflow event mean concentrations (EMCs) ranged from 0.1 to 1.2 mg/L; the highest EMC occurred in storm S3 (Table 1) and decreased thereafter. Outflow NH<sub>4</sub>+N concentrations varied for storms S3 through S7 (Kruskal-Wallis  $\chi 2 = 94.9$ , p<0.0001), with S3 > S4 and S5 > S6 and S7 (Dunn's test). Concentrations of  $NO_3^-$ N were low ( $\sim$ 0.1 mg/L) in dosing waters, but higher in outflows for storms S1 and S2 (6.5 to 75.8 mg/L), and also relatively high in storms S3 through S7 (2.1 to 7.6 mg/L), with EMCs ranging from 3.0 to 48.0 mg/L (Fig. 1b, Table 1). The increase in outflow NO<sub>3</sub>-N concentrations suggested leaching of NO<sub>3</sub> either previously formed or formed during a storm. Over time, NO<sub>3</sub>-N outflow concentrations decreased, with concentrations in storm S3 > S4 through S7 ( $\gamma$ 2 = 76.3, p < 0.0001), and with storms S4 and S6 > S5 and S7 (Dunn's test, p =0.011) (Fig. 1b). The decrease in  $NO_3^-$ N concentrations between storms S4 and S5, and between storms S6 and S7, could have resulted from increased outflow volumes and related dilution. During storms S4 or S6, a substantial amount of water was stored in the biofilter; in storms S5 or S7, more water was discharged (Fig. S5).

Mass flow rates were calculated to estimate the relative removal or export of NH $^+_4$ -N and NO $^-_3$ -N across storms. NH $^+_4$ -N mass flow rates exiting biofilter C4 peaked (22.1 mg/min) after the high NH $^+_4$ -N input from storm S3 (Fig. 2, a and b), while large NO $^-_3$ -N mass flow rates in biofilter output for storms S1 and S2 suggested NO $^-_3$  formation prior to the study. NO $^-_3$ -N mass flow rates ranged from 0 to 1220 mg/min, and 0 to 2.0 mg/min, in biofilter outputs and inputs, respectively (Fig. 2, c and d). Relative percent mass removal for NH $^+_4$ -N within a storm ranged from 60.7 to 92.3% and was lowest during storms S4 and S5. Organic N mineralization within the biofilter possibly contributed additional NH $^+_4$ -Also, NH $^+_4$  introduced with storm S3 could have been initially retained in a surficial organic layer observed after sewage-contaminated inflow drained from the biofilter. Subsequent sewage-free inflows would have eroded this layer and introduced NH $^+_4$  into the soil profile. Unlike NH $^+_4$ ,

NO<sub>3</sub> was exported for storms S1–7 (Fig. 2, c and d), with NO<sub>3</sub>-N mass export exceeding mass import by 3000% (Table 1).

In all storms except S3, the amount of NO<sub>3</sub>-N exported was an order of magnitude greater than either NO<sub>3</sub>-N or NH<sub>4</sub>+N inputs (Table 1) and could not be explained by nitrification of inflow NH<sub>4</sub>. The NO<sub>3</sub> exported during storms S3-7 may have formed following the high nutrient inputs in storm S3. Alternatively, the NO<sub>3</sub> existed in the biofilter soil prior to stormwater dosing. This would explain that the highest NO<sub>3</sub> concentrations and leaching occurred for storm S1. NO<sub>3</sub>-N export increased for consecutive storms S4 and S5 (antecedent dry period < 2 h) but decreased for storms S6 and S7 (antecedent dry period < 2 h), which may have indicated less NO3 leaching from the soil or more denitrification.  $NO_3^-$ -N mass export exceeded values reported for bioretention in the stormwater BMP database (Clary et al., 2011), with median and maximum NO3-N mass exports as a percentage of imports of 25% and 1500%, respectively (Valenca et al., 2021). NO<sub>3</sub> export thus resulted from leaching of pre-existing NO<sub>3</sub> (prior to storm S1), high hydraulic and nutrient loading in storm S3, and internal N processing.

Overall, concentration and mass flow data suggested biofilter retention of  $NH_4^+$  within a storm and export of  $NO_3^-$  formed between storms. The declining  $NO_3^-$  export after consecutive storms indicated some denitrification during storms S6 and S7. To further elucidate N fates, C processing, and redox conditions,  $CO_2$ ,  $CH_4$  and  $N_2O$  emissions were assessed.

# 3.4. Emissions of CO<sub>2</sub>, CH<sub>4</sub> and N<sub>2</sub>O in test biofilter C4

Test biofilter C4 emitted  $CO_2$ -C in the range of 79.5 to 239.7 mg/m²h, while mean values of  $142.2 \pm 44.4$  mg  $CO_2$ -C /m²h (Table S4, Fig. S6 a) were comparable to other biofilters (88.3 to 367.9 mg  $CO_2$ -C /m²h) (Grover et al., 2013, McPhillips et al., 2018). However, the measurements were made with shaded chambers, which precluded photosynthesis and  $CO_2$  uptake by plants and thus led to higher  $CO_2$  emissions. Plant root respiration likely also contributed to  $CO_2$  emissions (Baggs 2006). Highest  $CO_2$  emissions occurred after storm S3, which delivered high organic N and C amounts.  $CO_2$  emissions were linearly related with temperature ( $R^2 = 0.39$ , p = 0.02), likely from increased microbial respiration. There were no measurable  $CH_4$  emissions prior to wet-up, indicating that biofilters were a small  $CO_2$  sink via methanotrophy

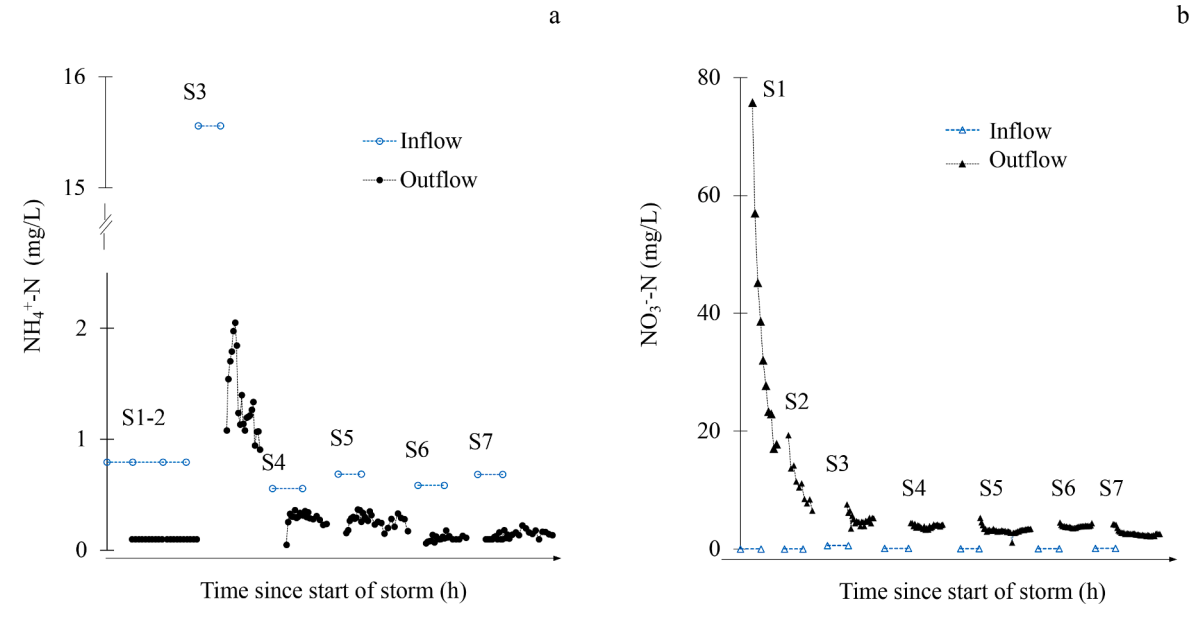


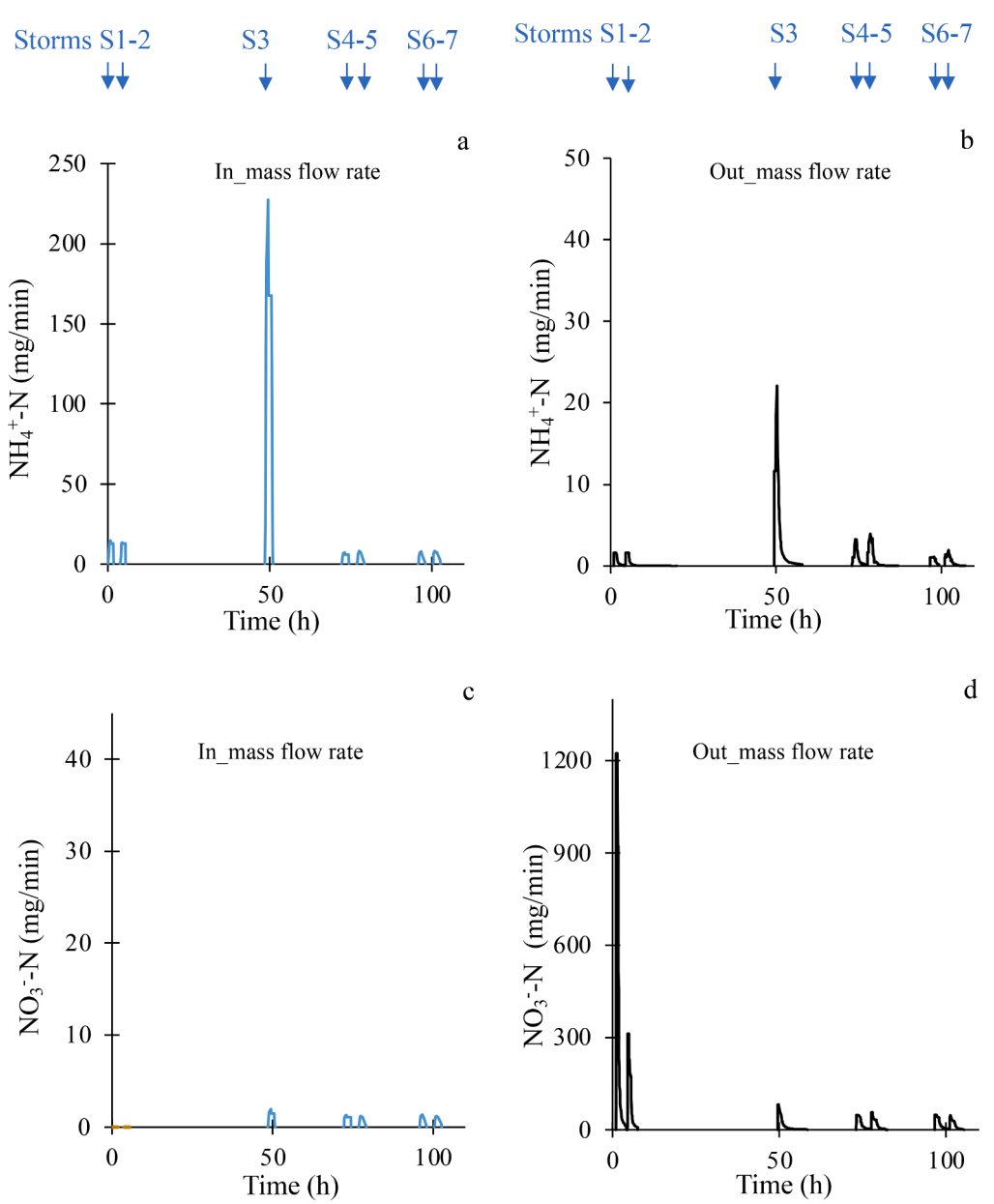
Fig. 1. Inflow and outflow concentration profiles for ammonium ( $NH_4^+$ -N) (a) and nitrate ( $NO_3^-$ -N) (b) in test biofilter C4 during storms S1 through S7. The time between storms has been shortened for visualization; actual timing for storms is shown in Fig. 2. The break in the y-axis in (a) from 2 mg/L to 15 mg/L allows visualizing the high inflow  $NH_4^+$ -N concentration during storm S3, corresponding to a 1:1 mix of sewage and stormwater runoff.

Table 1  $NH_4^+$ -N and  $NO_3^-$ N event mean concentrations, masses, and relative removal in inflows and outflows of test biofilter C4 for storms S1 through S7.

	<b>S1</b>	<b>S2</b>	S3	<b>S4</b>	S5	<b>S</b> 6	<b>S7</b>
NH <sub>4</sub> +N							
EMC inflow (mg/L) <sup>a</sup>	0.79	0.79	15.6	0.55	0.69	0.58	0.68
EMC outflow (mg/L)	0.10	0.10	1.21	0.21	0.24	0.1	0.13
Reduction (%)	87.5	89.4	92.2	58.2	64.9	81.6	80.3
Mass input (g)	1.13	1.07	21.0	0.78	0.96	0.82	0.93
Mass output (g)	0.11	0.13	1.58	0.28	0.38	0.13	0.20
Removal (%)	90.0	87.7	92.3	64.1	60.7	84.1	78.4
NO <sub>3</sub> -N							
EMC inflow (mg/L)	< MDL	< MDL	0.13	0.10	0.10	0.10	0.10
EMC outflow (mg/L)	48.0	11.8	5.39	4.06	3.56	4.06	2.97
Reduction (%) <sup>b</sup>	na	na	-3920	-3961	-3461	-3960	-2874
Mass input (g)	0.0	0.0	0.18	0.14	0.14	0.14	0.14
Mass output (g)	54.8	18.5	7.05	5.03	5.52	5.01	4.35
Removal (%)	na	na	-3880	-3470	-3820	-3480	-3080

<sup>&</sup>lt;sup>a</sup> EMC is the event mean concentration, equivalent to total mass divided by total volume. Reductions in EMC, and mass removal are calculated relative to the inflow. See Fig. 1 for time-course plots of  $NH_4^+$ -N and  $NO_3^-$ -N concentrations for each storm.

<sup>&</sup>lt;sup>b</sup> For  $NO_3^-N$  in storms S1 and S2, calculations were not performed because inflows were below the method detection limit (MDL) (0.1 mg/L). See Section 2.3 for method and MDL details.



**Fig. 2.** Mass flow rates for NH $_4^+$ -N inflow (a) and outflow (b) and NO $_3^-$ N inflow (c) and outflow (d) in test biofilter C4 for storms S1 through S7 (blue arrows in top panel). Note scale differences on y-axis for all panels. In (c), there was no measurable NO $_3^-$ N in the inflows of storms S1 and S2. For each storm, the outflow NH $_4^+$ -N mass rate is lower than the inflow mass rate (and b). A large pulse of previously formed NO $_3^-$ N is released during storms S1–2, but for all storms the outflow NO $_3^-$ N exceeds the inflow mass rate (c and d).

when soils were dry, as observed by others (Grover et al., 2013). After dosing, the biofilter was a CH<sub>4</sub> source, with emissions ranging from 10.2 to 205.5 µg CH<sub>4</sub>-C /m<sup>2</sup> h (Fig. S6 b, Table S4), and with mean emissions  $(116.3 \pm 83.1 \,\mu g \, CH_4 - C \, /m^2 \, h)$  higher than other biofilters ( -11.1 to 45.5  $\mu$ g CH<sub>4</sub>-C/m<sup>2</sup> h) (Grover et al., 2013, McPhilips et al. 2018), likely due to differences in inflows and draining times and in how CH4-C emissions were measured. Specifically, sewage addition during storm S3 introduced large amounts of decomposable C, which can promote CH<sub>4</sub> production (Cao et al., 1996). CH<sub>4</sub>-C emissions increased as wetting progressed (Fig. S6b) and positively correlated with soil saturation (Pearson's r = 0.84, p = 0.0001) but negatively correlated to the antecedent dry period (Pearson's r = -0.71, p = 0.006). CH<sub>4</sub>-C emissions confirmed methanogenesis, and thus that soils were anoxic. Methanogenesis proceeds under deeply reducing conditions, which occur when NO<sub>3</sub> depletes (Achtnich et al., 1995). Thus, CH<sub>4</sub>-C emissions were indicative of NO<sub>3</sub> depletion via denitrification.

Biofilter C4 was an  $N_2O$  source, with mean emissions of 48.7  $\pm$  25.4  $\mu$ g N<sub>2</sub>O-N/m<sup>2</sup> h, and values ranging from 12.8 to 84.3  $\mu$ g N<sub>2</sub>O-N/m<sup>2</sup> h (Table S4, Fig. 3), higher than detention basins (0.5 to 9.5  $\mu$ g N<sub>2</sub>O-N/m<sup>2</sup> h) (McPhillips and Walter 2015) and infiltration basins (means of 1.1 and 34.3 µg N<sub>2</sub>O-N /m<sup>2</sup> h) (Morse et al., 2017), but comparable to parking lot biofilters (13.7 to 65.6  $\mu$ g N<sub>2</sub>O-N/m<sup>2</sup> h) (Grover et al., 2013). Mean N2O-N emissions across storms were similar, and comparable to baseline measurements (Fig. 3a). However, sampling occurred after standing water had drained, i.e., after maximum N2O emissions and with reoxygenation. N2O-N emissions increased prior to dosing and declined after wetting when the biofilter was more saturated (Fig. 3b). This trend was confirmed by the positive correlation between N<sub>2</sub>O-N emissions and antecedent dry period (Pearson's r = 0.61, p = 0.027) and the negative correlation with soil saturation (Pearson's r = -0.59, p = 0.027). The biofilter was briefly waterlogged and saturation was mostly below 70% (for 92 h of the 110 h timeseries) (Fig. S5c); thus, N2O emissions were from nitrification and also denitrification (in anaerobic microsites; Parkin 1987). Decreased N<sub>2</sub>O-N emissions following dosing may have owed to more N2O conversion to N2 as gas slowly diffused through the saturated biofilter. Contrariwise, gas transport through dry soils is faster, thereby increasing N2O emissions. Also, enzymes catalyzing N2O

reduction to  $N_2$  are sensitive to  $O_2$  levels such that, as soil dries and  $O_2$  levels increase,  $N_2O$  reduction is inhibited (Philippot et al., 2007).  $N_2O$ -N emissions following storm S3 (sewage-contaminated runoff) remained relatively high (Fig. 3a), likely due to increased soil respiration with C inputs (storm S3), creating localized anaerobic microsites promoting denitrification (Parkin 1987).

Overall,  $CO_2$ -C and  $CH_4$ -C emissions suggested both oxic and anoxic biofilter soil redox conditions, while  $N_2O$ -N emissions indicated that nitrification and denitrification were co-occurring and influenced by soil water content, soil temperature, and C and N supply. To further investigate N processes,  $NO_3^-$  isotopic ratios were evaluated.

# 3.5. Dual NO<sub>3</sub> isotopic ratios analysis

Stable NO<sub>3</sub> isotopic ratios ( $\delta^{18}\text{O-NO}_3$  and  $\delta^{15}\text{N-NO}_3$ ) were determined for storms S3 through S7 inflows and outflows, and for biofilter C4 soil eluates. Outflow samples were most depleted in  $\delta^{18}$ O-NO<sub>3</sub> and  $\delta^{15}$ N-NO<sub>3</sub>, ranging from -17.1 to 3.7 ‰, and -9.8 to 9.7 ‰, respectively, followed by soil eluates, and inflow samples, which were enriched relative to outflows (+15% for  $\delta^{15}$ N-NO $_3^-$ , +30% for  $\delta^{18}$ O- $NO_3^-$ ) (Fig. 4, Table S5). The  $\delta^{18}O$ - $NO_3^-$  and  $\delta^{15}N$ - $NO_3^-$  of inflows, outflows, and soil eluates were compared against common NO<sub>3</sub> sources (Kendall et al., 2007; Hastings et al., 2013). Inflow samples were similar to septic waste in their  $\delta^{15}$ N-NO $_3^-$  enrichment but not in their oxygen enrichment. Soil  $\delta^{15}$ N-NO $_3^-$  eluate values were midway between inflow samples and septic waste, comparable to stormwater and septic waste  $NO_3^-$  mixtures. Outflow  $\delta^{18}O$ - $NO_3^-$  values corresponded to  $NO_3^-$  sources from nitrification (Fig. 4) (Kendall et al., 2007). Such nitrification evidence was consistent with decreasing NH<sub>4</sub><sup>+</sup> concentrations and increasing NO<sub>3</sub> concentrations from inflows to outflows (Fig. 1, Table 1). The depletion in  $\delta^{18}\text{O-NO}_3^-$  and  $\delta^{15}\text{N-NO}_3^-$  from inflow to outflow (Fig. 4, top right and bottom left, respectively) was also consistent with nitrification. Nitrifying bacteria derive their N isotopic signatures from NH<sub>4</sub> and their O isotopic values from water and atmospheric O<sub>2</sub> at a ratio of 2/3 H<sub>2</sub>O to 1/3 O<sub>2</sub> (Kendall and McDonnell 2012). Overall, nitrification depletes  $\delta^{18}$ O-NO<sub>3</sub> because water is more depleted in  $^{18}$ O than in the atmosphere; nitrification depletes  $\delta^{15}$ N-NO<sub>3</sub>

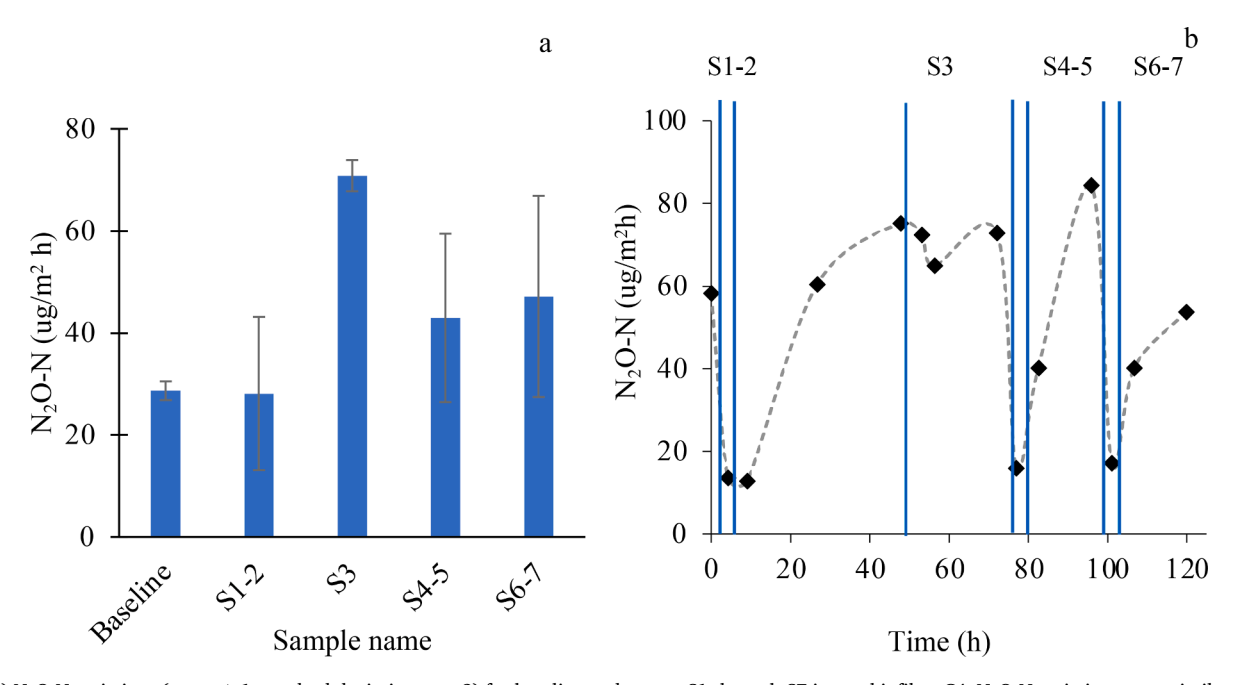


**Fig. 3.** a)  $N_2O$ -N emissions (mean  $\pm$  1 standard deviation, n=3) for baseline and storms S1 through S7 in test biofilter C4.  $N_2O$ -N emissions were similar (Kruskal-Wallis, p>0.05). b)  $N_2O$  emissions trends for storms S1 through S7 (blue lines). Time zero corresponds to the first  $N_2O$  sampling prior to storm S1 dosing. There were three measurements per dosing day, one measurement in between storms S2 and S3, and one measurement the day after storm S7. Trends in between measurements were inferred (dashed lines) but suggested dampened  $N_2O$  emissions following a storm, except for storm S3.

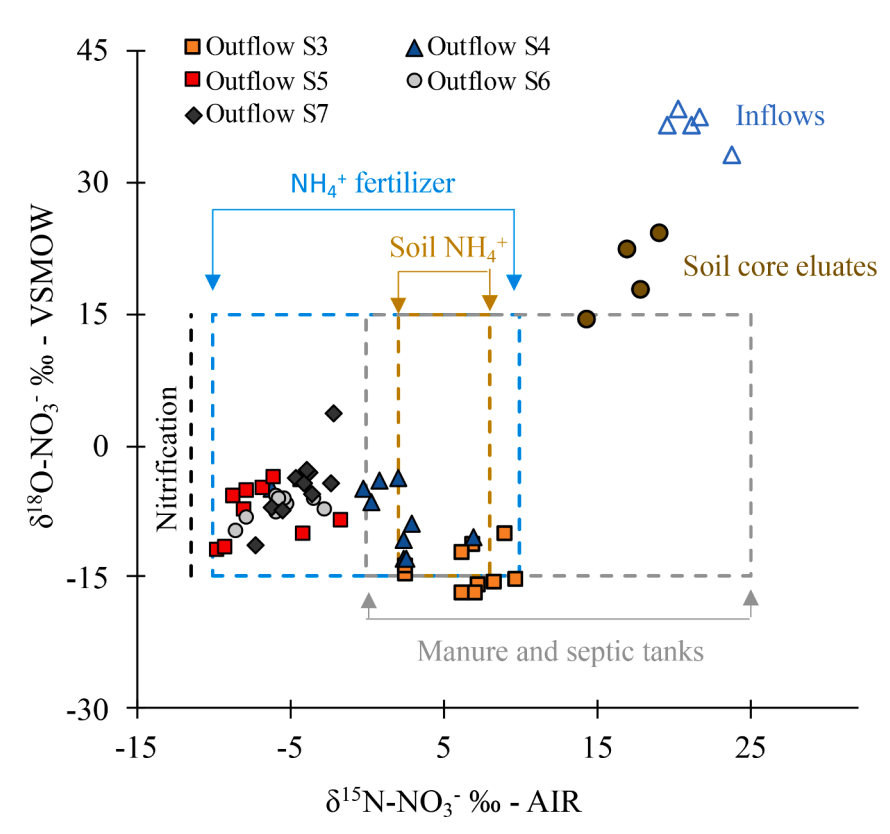


Fig. 4. Nitrate isotopic ratios ( $\delta^{18}\text{O-NO}_3^-$  and  $\delta^{15}\text{N-NO}_3^-$ ) for inflows and outflows (storms S3 through S7), and soil eluates for test biofilter C4. Also shown are typical  $\delta^{18}\text{O-NO}_3^-$  for nitrate from nitrification of ammonium, denoted by "Nitrification", as isotopic composition areas for these NH $_4^+$  sources: ammonium fertilizers, soil ammonium, and manure and septic waste (Kendall et al., 2007; Hastings et al., 2013).  $\delta^{18}\text{O-NO}_3^-$  and  $\delta^{15}\text{N-NO}_3^-$  are reported relative to Vienna Standard Mean Ocean Water (VSMOW), and N $_2$  in air (AIR), respectively.

because lighter molecules are preferentially nitrified. Average  $\delta^{15}\text{N-NO}_3^-$  values decreased between S3 and S5 (Kruskal-Wallis  $\chi 2=35.48,\,p<0.001;$  Dunn's test, p<0.001), and were similar for storms S5 through S7 (Fig. S7a) indicating competing processes of N assimilation and denitrification (Sigman et al., 2005). Average  $\delta^{18}\text{O-NO}_3^-$  for storms S3 through S7 differed ( $\chi 2=24.29,\,p<0.001$ ) due to enrichment from storms S3 to S4 (Dunn test, p<0.01) (Fig. S7b) owing to  $^{18}\text{O}$  enrichment during evaporation in upper soil layers, and preferential consumption of  $^{16}\text{O}$  when plants and microbes respire (Spoelstra et al., 2007). The longer draining time between storms S3 and S4, and the increased respiration following high nutrient inputs in storm S3, support these interpretations since  $\delta^{18}\text{O-enriched NO}_3^-$  would be flushed by incoming water.

In later storms, denitrification was evidenced: outflow  $\delta^{18}$ O-NO $_3^-$  and  $\delta^{15} \text{N-NO}_3^-$  for storms S6 and S7 were linearly related, with slopes between 0.5 and 1 (Sigman et al., 2005); this relationship was significant for storm S7 ( $R^2 = 0.84$ , p = 0.002) (Fig. S7c). Isotopic evidence for denitrification was also investigated in endpoint soil core eluates. Since infiltration partially displaces stored water, surface soils would contain younger, more oxygenated water while deep soils would have older, less oxygenated water, such that denitrification would be favored with depth. This would result in enriched  $\delta^{18} \text{O-NO}_3^-$  and  $\delta^{15} \text{N-NO}_3^-$  with depth, as confirmed by the positive linear relationship ( $R^2 = 0.68$ , slope = 1.83, p = 0.18) (Fig. S7d). The slope > 1 implied that other processes intervened in NO<sub>3</sub> removal, such as N assimilation, which has a similar isotopic signature to denitrification (Sigman et al., 2005). N assimilation by biofilter plants, a common fate for NO<sub>3</sub> (Payne et al. 2014b) may explain the observed slope between  $\delta^{18}\text{O-NO}_3^-$  and  $\delta^{15}\text{N-NO}_3^-$ . If assimilated N is mineralized to NH<sub>4</sub><sup>+</sup> and then nitrified,  $\delta^{18}\text{O-NO}_3^-$  values increase further (Sigman et al., 2005).

Overall, isotope data supported that nitrification dominated, while denitrification occurred in later storms when soils were more saturated. Other suggested N fates were assimilation coupled with remineralization. To confirm the potential for nitrification and denitrification, soil nitrifying and denitrifying bacterial gene abundances were evaluated.

# 3.6. qPCR and 16S rRNA gene sequencing

All qPCR assays had amplification efficiencies between 85.2% and 103.1% with an  $R^2$  greater than 0.99. Nitrifier and denitrifier bacterial genes co-existed throughout the soil profile, showing depth-dependent enrichment, as detailed below. While qPCR analyses were based on one composite sample for each soil depth, and thus the significances of depth-related gene copy trends could not be determined, there were apparent differences.

The 16S rRNA gene abundances were comparable to other biofilters (Chen et al., 2013), with values ranging from  $9.2 \times 10^8$  to  $5.7 \times 10^9$  gene copies per gram of dry soil (gc/g dry soil) (Fig. 5a,b; Table S6). Copies of genes encoding 16S rRNA appeared to increase between the surface (0-10 cm) and 10 to 20 cm soil sections, and decrease with soil depth thereafter (Fig. 5a and Table S6). Bacterial and archaeal ammonia oxidizing (amoA) gene abundances ranged from  $1.2 \times 10^3$  to  $2.3 \times 10^4$ and  $2.1 \times 10^5$  to  $1.2 \times 10^6$  gc/g dry soil, respectively (Fig. 5a,b; Table S6). Bacterial amoA gene abundance was comparatively low; for example, field-based biofilters average per dry gram of soil 10<sup>4</sup> to 10<sup>6</sup> copies, while biofilter columns typically have 10<sup>6</sup> to 10<sup>8</sup> amoA gene copies (Chen et al., 2013; Chen et al., 2019). However, values measured here are similar to pristine and agricultural soils ( $\sim 10^3$  to  $10^7$  per dry soil gram; Leininger et al., 2006). Archaeal amoA gene copies were comparable to agricultural soils (10<sup>4</sup> to 10<sup>8</sup> per dry soil gram) (Leininger et al., 2006). At every sampled depth, archaeal amoA genes were 10 to 900 times more abundant than bacterial amoA, similarly to others (Leininger et al., 2006). Archaeal amoA gene prevalence suggests that ammonia oxidizing archaea may have contributed significantly to biofilter nitrification. Copies of the amoA gene normalized to 16S rRNA gene copies showed an apparent increase with depth for archaeal amoA in C2, and bacterial amoA in C4 (Fig. S9), suggesting different niche preferences (Table S2).

Denitrifiers were assessed via the *nir*K, *nir*S, and *nos*Z genes, whose abundances ranged from  $4.5 \times 10^5$  to 3.1 to  $10^6$ ,  $1.8 \times 10^6$  to  $1.5 \times 10^7$ , and  $5.0 \times 10^5$  to  $2.2 \times 10^6$  gc/g dry soil, respectively (Fig. 5a,b;

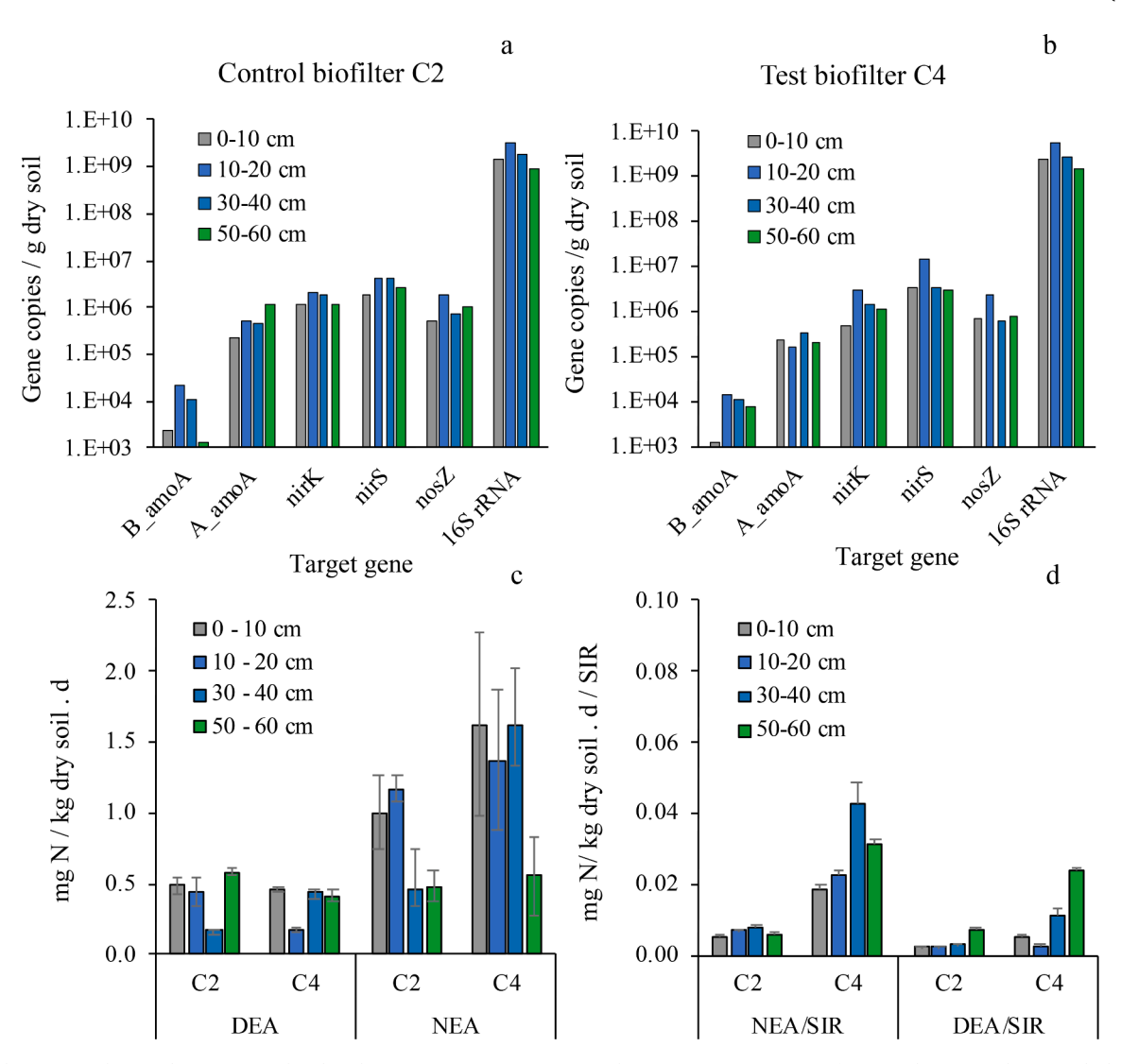


Fig. 5. Total 16S rRNA, bacterial (B\_amoA) and archaeal (A\_amoA) amoA, nirS, and nosZ gene concentrations for control C2 (a) and test C4 (b) biofilter soils. Each composite sample was sectioned at 0 to 10 cm, 10 to 20 cm, 30 to 40 cm, and 50 to 60 cm, and subsampled in triplicate to extract DNA, which was then pooled. The average gene copies for each pooled sample are graphed. Bottom panels: mean and range (n=2) for nitrifying (NEA) and denitrifying (DEA) enzyme activities (c), and the NEA and DEA normalized to microbial biomass by substrate induced respiration (SIR) (d), of duplicate subsamples of the same composites from a) and b). The "d" in the y-axes for the bottom panels refers to "day".

Table S6), and were similar to other biofilters (nirK:  $10^4$  to  $10^8$ ; nirS:  $10^5$  to  $10^8$ ; nosZ:  $10^5$  to  $10^8$  gc/g dry soil) (Chen et al., 2013; Waller et al., 2018). Denitrifier gene abundances generally decreased with depth (Fig. 5a,b), paralleling overall 16S rRNA gene copies. When normalized to 16S rRNA gene copies, denitrifying genes increased with depth for C2; this trend was apparent for nirK in C4 (Fig. S9).

Results from previously reported (Li et al., 2021) 16S rRNA gene sequences in these biofilter soils were used to estimate the relative abundance of autotrophic nitrifiers. Major assigned bacterial phyla were  $\alpha$ -,  $\beta$ -,  $\gamma$ -, and  $\delta$ - Proteobacteria, Acidobacteria Actinobacteria, Bacteroidetes, Chloroflexi, and Nitrospirae (Fig. S10). The *Nitrospira* genus includes soil nitrite-oxidizing bacteria (NOB) and was relatively abundant in biofilter soil, ranging from 0.80 to 2.10% in test biofilter C4, and 0.57 to 1.50% in control biofilter C2, which was comparable to biofilter mesocosms (0.005 to 2%) (Morse et al., 2018). The relative abundance of *Nitrospira* increased with soil depth (Fig. S10). Other identified genera were *Nitrosomonas*, and *Nitrobacteria* for NOB, and *Nitrosopumilus* for ammonia oxidizing archaea.

# 3.7. Nitrifying and denitrifying enzyme activities

Potential enzyme activities were measured to indicate nitrifying and denitrifying bacterial population sizes. NEA in biofilters C2 and C4 ranged from 0.45 to 1.63 µg N/g dry soil/day (Fig. 5c) and decreased with soil depth. When NEA results were normalized to SIR, nitrification potentials were uniform in C2 and increased with depth in C4 (Fig. 5d), indicating higher relative abundance of nitrifiers with depth, consistent with qPCR results (Fig. S9b). However, NEA, and archaeal and bacterial amoA were not significantly related. Near the surface, NEA was larger than DEA, but in the 30 to 40 cm and 50 to 60 cm soil sections NEA and DEA were similar, suggesting comparable nitrification and denitrification potentials at depth. DEA ranged from 0.17 to 0.59  $\mu$ g N/g dry soil/ day (Fig. 5d) and was on the lower end for biofilters and bioretention basins (0.24 to 16.8 µg N/g dry soil/day) (Morse et al., 2017; Waller et al., 2018; Kavehei et al., 2021). The lower DEA values observed herein may be a result of design differences (e.g., biofilters vs. retention basins that remain wet), a relatively drier climate, and a younger biofilter age. DEA normalized to SIR increased with depth in C4, suggesting more favorable denitrification conditions, consistent with NO3 isotope results. DEA was negatively correlated to *nir*K (Spearman's  $\rho = -0.72$ , p =

0.054) and *nir*S (Spearman's  $\rho=-0.70,\ p=0.042),$  indicating a disconnect between denitrifier abundance and activity.

## 3.8. Transport timescales and biological reaction rates

Transport timescales and biological reaction rates were compared to evaluate if biofilter residence time allowed biological transformation within, and between, storms. Transport times were determined from the mean age of water stored in the biofilter, as developed previously (Parker et al., 2021). Mean water ages ranged from 7.3 to 29.5 h for storms S1 through S7, and 9.3 to 27.1 h between storms (Fig. S8). N mineralization reaction constants,  $k_{min}$ , and reaction times,  $\tau_{min}$ , were derived from ecosystem respiration rates (Fig. S6a, Table S4) and soil data (Supplemental Methods), assuming that total mineralizable N was 5 to 20% of TN. Average k<sub>min</sub> ranged from 0.002 to 0.008 day<sup>-1</sup>, which was comparable to other soil studies (0.001 to 0.004 day<sup>-1</sup>) (Lotse et al., 1992). N mineralization times ranged from 18 to 100 weeks. For nitrification, reaction rate constants derived from soil and bioretention studies ranged from 0.02 to 0.5 day<sup>-1</sup> (reaction times: 2 to 50 days) (Lotse et al., 1992; Chen et al., 2019), which were similar or faster than those reported for denitrification, ranging from 0.01 to 0.2 day<sup>-1</sup> (reaction time: 5 to 100 days) (Lotse et al., 1992; Chen et al., 2019; Kavehei et al., 2021). Denitrification may be slower than nitrification in aerated soils because higher O2 levels promote aerobic processes (Schlesinger 2009). The water age ranges (hours to days) and biological reaction times (days to months) confirmed N processing dynamics expected for fast draining biofilters: dominance of transport during storms, and

enhanced biological reactions during drying periods. Denitrification during dry periods, however, would be limited due to  $O_2$  competing as a terminal electron acceptor.

### 3.9. Mass balance of $NH_4^+$ -N, $NO_3^-$ -N and $N_2$ O-N emissions

A partial mass balance of  $NH_4^+$ -N,  $NO_3^-$ -N, and  $N_2O$ -N emissions for storms S3 through S7 suggested that test biofilter C4 was removing  $NH_4^+$  from the inflow (negative aqueous  $NH_4^+$ -N delta) and acting as a net nitrifier (positive soil and aqueous  $NO_3^-$ -N deltas) (Fig. 6). The soil  $NH_4^+$ -N balance was positive, suggesting that N mineralization and  $NH_4^+$  adsorption from inflow stormwater dominated over plant uptake, microbial immobilization, and nitrification. Although nitrification dominated over denitrification, N mineralization and  $NH_4^+$  adsorption may have been more important processes because nitrifiers only represented a small fraction of total bacteria, and nitrification time scales were long.

The NH $_4^+$ -N mass introduced with storm S3 (21.0 g N, Table 1) was an order of magnitude greater than soil NH $_4^+$ -N mass prior to S3 (3.66 g N, Table S7), while soil NO $_3^-$ -N (7.93 g N, Table S7) was an order of magnitude greater than NO $_3^-$ -N inputs in S3 (0.18 g N, Table 1). NH $_4^+$  temporarily retained during S3 (subtracting output from input: 19.4 g N, Table 1) was similar to the excess NO $_3^-$ -N leaving the biofilter during storms S4 through S7 (subtracting inputs from outputs:19.6 g N, Table 1). These results suggested that NH $_4^+$  retained within a storm was nitrified in between storms (ca. 1 day herein) and released as NO $_3^-$  in later storms. However, most NO $_3^-$  export occurred during conditioning storms (S1–2) (Fig. 2), likely from NO $_3^-$  formed in the preceding dry

IN – OUT + Production (P) – Consumption (C) = 
$$\Delta M_{soil}$$

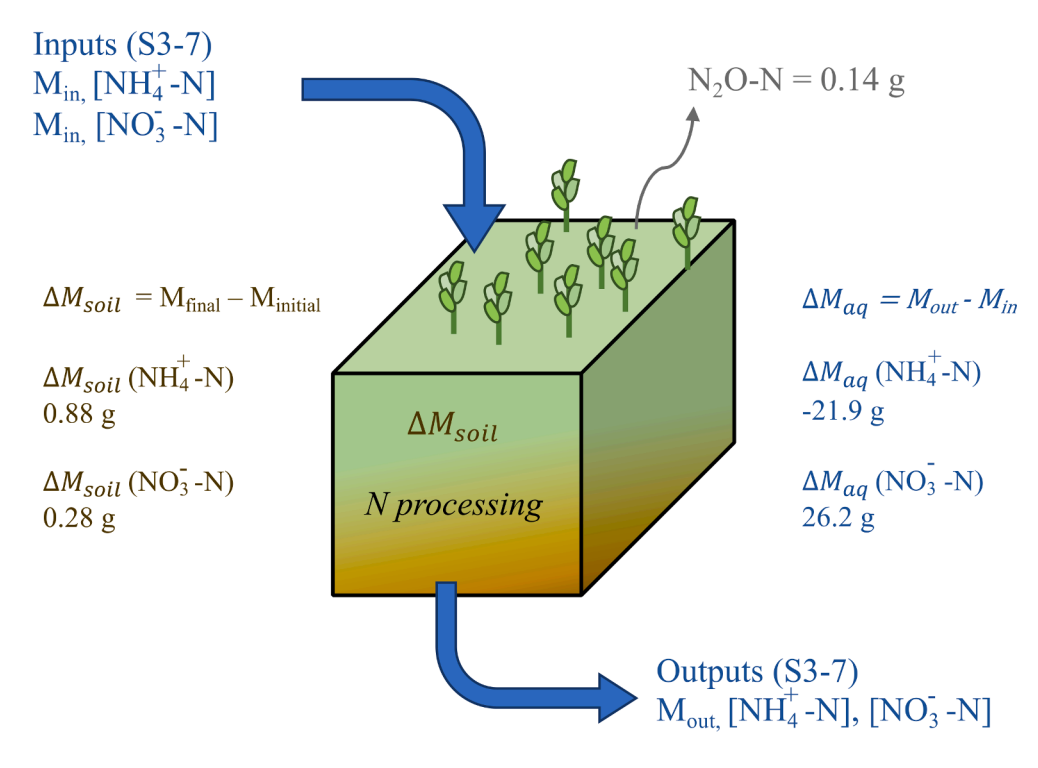


Fig. 6. Conceptual diagram and equations for a partial mass balance of NH<sub>4</sub>+N, NO<sub>3</sub>-N and N2O-N in biofilter C4 for storms S3-7. The mass balance shown here accounts for 54% lateral aqueous exfiltration (Parker et al., 2021). Soil masses of N species were approximated from C2 cores prior to storm S3 (initial), and C4 cores after storm S7 (final). The negative delta for aqueous NH<sup>‡</sup>-N indicated retention in soil, but the relatively small positive delta for soil NH<sub>4</sub><sup>+</sup>-N suggested a large portion of the retained NH<sub>4</sub> was assimilated and/or nitrified. The positive deltas for soil and aqueous NO3-N suggested the biofilter was a net nitrifier. The N2O-N mass emission was approximately an order of magnitude lower than changes in NH<sub>4</sub>+N and NO<sub>3</sub>-N.

$$(P - C)_{NH_4 - N}^{+} = \Delta M_{soil}(NH_4^{+} - N) + \Delta M_{aq}(NH_4^{+} - N) = -21.0 g$$

$$(P - C)_{NO_3^{-} - N}^{+} = \Delta M_{soil}(NO_3^{-} - N) + \Delta M_{aq}(NO_3^{-} - N) = 26.5 g$$

period; similarly, previously formed  $NO_3^-$  may have also contributed to the  $NO_3^-$  export in storms S3–7. The relatively low  $N_2O$ -N emissions (0.014 g N) could not differentiate between the two possibilities of minimal denitrification or complete denitrification when it occurred.

When considering  $NO_3^-N$ , soil storage increased by 0.28 g N, while the balance of aqueous flows exported 26.2 g N (Fig. 6), suggesting that assimilation and denitrification were not as significant as nitrification. Between storms, inflow and stored  $NH_4^+$  nitrification may have formed  $NO_3^-$ . When soils were re-wet,  $NO_3^-$  leaching commenced and persisted during subsequent storms. These results highlight the importance of monitoring biofilter outflow following a high-flow, and high-loading, storm event, since N export may persist in successive storms. This N export would depend on inflow characteristics, soil properties, biofilter vegetation, and biofilter designs. Still, biofilters that rapidly infiltrate runoff are almost certain to be hydraulically overloaded when experiencing large, pulsed storms, and thus would not support N removal via denitrification.

### 4. Conclusion and recommendations

A full-scale biofilter was pulsed with unpolluted stormwater then challenged with a large pulse of N (mainly NH<sub>4</sub>) and other sewageassociated nutrients (e.g., organic C) during realistic simulated storms; successive storms flushed, delivering relatively unpolluted stormwater. All storms resulted in NO<sub>3</sub> leaching. The inflow NH<sub>4</sub> pulse underwent all expected soil system fates: adsorption, assimilation by plants, immobilization by microbes, and nitrification. However, the NO<sub>3</sub> mass released from the biofilter exceeded what could have been formed by nitrification of NH<sub>4</sub> added during the large pulse (storm S3), partly from NO<sub>3</sub> that had accumulated in biofilter pore fluids prior to the experiment. The estimates for mineralization, nitrification, and denitrification reaction times were longer than biofilter residence times during storms, but supported N transformations during storms, thus favoring NO<sub>3</sub> production between storms and NO3 leaching during storms. Via a comprehensive analysis of chemical, bacterial, and isotopic metrics, denitrification was shown to be limited for high-frequency, large storms; thus, the biofilter was a net  $NO_3^-$  exporter.

Typical pass-through biofilters perform poorly, in terms of removing N, when challenged with large, pulsed storms. To promote denitrification and permanent N removal, residence times would have to increase from hours to days, which may be problematic because high hydraulic conductivity is needed for rapid infiltration, and longer residence times may also favor methanogenesis and CH<sub>4</sub> release. Further, design guidelines recommend not exceeding drawdown times of 24 to 72 h (Sage et al., 2015) to avoid overflows and prolonged ponding (Le Coustumer et al., 2012). A viable way of addressing the mismatch between reaction and residence times may be a treatment train consisting of a stormwater capture system (e.g., using real-time control to optimize runoff capture (Parker et al., 2022)), followed by fast- and slow-draining cells. The tank reduces off-site runoff, the first cell reduces runoff volume, and the second cell enhances N removal by prolonging contact times. As such, inflow NH<sub>4</sub><sup>+</sup> is adsorbed and nitrified in the first cell, while inflow NO<sub>3</sub> and DON flow into the second cell. Longer residence times promote denitrification and NO3 removal, while clay minerals in soils sorb DON (Wang et al., 2020). Although DON can be mineralized and nitrified, by separating inflow NH<sub>4</sub> and DON in the first and second cell, respectively, a larger N pulse is transformed into two smaller and more manageable pulses, supporting lower N export from biofilters.

# **Declaration of Competing Interest**

The authors declare the following financial interests/personal relationships which may be considered as potential competing interests:

# Data availability

Data will be made available on request.

# Acknowledgments

This research was supported by funding from by the University of California Office of the President, Multicampus Research Programs and Initiatives, Grant ID MRP-17-455083. EAP and SBG were additionally supported by an NSF Growing Convergence Research (GCR) award (#2021015). We thank Jian Peng, and the Orange County Public Works, CA for use of biofilters and onsite laboratory, logistical support, water filtration, and soil coring. We thank Beta Analytic Inc. and Source Molecular Corporation, particularly Florencia Goren and Thierry Tamers for financial support, and Zeneida Cernada and the IRMS team for technical assistance and analysis of nitrate isotopic ratios. Raw sewage was from the Orange County Sanitation District, CA. Nitrate analysis was performed at UC Riverside, with assistance from Emily Santiago. Dr. Jen Le assisted with GHG sampling. Plasmid DNA standards were provided by Dr. Alyson Santoro and Dr. Brian Badgley. Financial support from Mr. Henry H. Wheeler, Jr. is acknowledged.

# Supplementary materials

Supplementary material associated with this article can be found, in the online version, at doi:10.1016/j.watres.2022.119501.

#### References

- Achtnich, C., Bak, F., Conrad, R, 1995. Competition for electron donors among nitrate reducers, ferric iron reducers, sulfate reducers, and methanogens in anoxic paddy soil. Biol. Fertil. Soils 19 (1), 65–72.
- Baggs, E.M., 2006. Partitioning the components of soil respiration: a research challenge. Plant Soil 284, 1–5.
- Bratieres, K., Fletcher, T.D., Deletic, A., Zinger, Y., 2008. Nutrient and sediment removal by stormwater biofilters—a large-scale design optimisation study. Water Res. 42 (14), 3930–3940.
- Brown, R.A., Hunt, W.F., 2011. Impacts of media depth on effluent water quality and hydrologic performance of undersized bioretention cells. J. Irrig. Drain. Eng. 137 (3), 132–143
- Brown, R.A., Birgand, F., Hunt, W.F., 2013. Analysis of consecutive events for nutrient and sediment treatment in field-monitored bioretention cells. Water Air Soil Pollut. 224 (6), 1–14.
- Burgis, C.R., Hayes, G.M., Zhang, W., Henderson, D.A., Macko, S.A., Smith, J.A., 2020. Tracking denitrification in green stormwater infrastructure with dual nitrate stable isotopes. Sci. Total Environ. 747, 141281.
- Cao, M., Marshall, S., Gregson, K., 1996. Global carbon exchange and methane emissions from natural wetlands: Application of a process-based model. J. Geophys. Res. Atmos., 101(D9), 14399–14414.
- Chen, X., Peltier, E., Sturm, B.S., Young, C.B., 2013. Nitrogen removal and nitrifying and denitrifying bacteria quantification in a stormwater bioretention system. Water Res. 47 (4), 1691–1700.
- Chen, T., Liu, Y., Zhang, B., Sun, L., 2019. Plant rhizosphere, soil microenvironment, and functional genes in the nitrogen removal process of bioretention. Environ. Sci. Process. Impacts 21 (12), 2070–2079.
- Clary, J., Leisenring, M., Poresky, A., Earles, A., Jones, J., 2011. BMP performance analysis results for the international stormwater BMP database. In: Proceedings of World Environmental and Water Resources Congress. Reston, VA: ASCE.
- Davis, A.P., Shokouhian, M., Sharma, H., Minami, C., 2001. Laboratory study of biological retention for urban stormwater management. Water Environ. Res. 73, 5–14.
- Davis, A.P., 2007. Field performance of bioretention: water quality. Environ. Eng. Sci. 24 (8), 1048–1064.
- Grover, S.P.P., Cohan, A., Chan, H.S., Livesley, S.J., Beringer, J., Daly, E., 2013. Occasional large emissions of nitrous oxide and methane observed in stormwater biofiltration systems. Sci. Total. Environ. 465, 64–71.
- Hastings, M.G., Casciotti, K.L., Elliott, E.M., 2013. Stable isotopes as tracers of anthropogenic nitrogen sources, deposition, and impacts. Elements 9 (5), 339–344.
- Hatt, B.E., Fletcher, T.D., Deletic, A., 2009. Hydrologic and pollutant removal performance of stormwater biofiltration systems at the field scale. J. Hydrol. 365 (3), 310–321.
- Hunt, W.F., Jarrett, A.R., Smith, J.T., Sharkey, L.J., 2006. Evaluating bioretention hydrology and nutrient removal at three field sites in North Carolina. J. Irrig. Drain. Eng. 132 (6), 600–608.

- Kavehei, E., Farahani, B.S., Jenkins, G., Lemckert, C., Adame, M., 2021. Soil nitrogen accumulation, denitrification potential, and carbon source tracing in bioretention basins. Water Res., 116511
- Kendall, C., McDonnell, J.J., 2012. Isotope Tracers in Catchment Hydrology. Elsevier Science, Amsterdam, The Netherlands.
- Kendall, C., Elliott, E.M., Wankel, S.D. (2007). Chapter 12, tracing anthropogenic inputs of nitrogen to ecosystems. In: Stable Isotopes in Ecology and Environmental Science, 2nd ed., Lajtha, K., and Michener, R.H. (Eds.), Blackwell Scientific Publications, Oxford. UK.
- Le Coustumer, S., Fletcher, T.D., Deletic, A., Barraud, S., Poelsma, P., 2012. The influence of design parameters on clogging of stormwater biofilters: a large-scale column study. Water Res. 46 (20), 6743–6752.
- Leininger, S., Urich, T., Schloter, M., Schwark, L., Qi, J., Nicol, G.W., Prosser, J.I., Schuster, S.C., Schleper, C., 2006. Archaea predominate among ammonia-oxidizing prokaryotes in soils. Nature 442, 806–809.
- Li, L., Davis, A.P., 2014. Urban stormwater runoff nitrogen composition and fate in bioretention systems. Environ. Sci. Technol. 48 (96), 3403–3410.
- Li, D., Van De Werfhorst, L.C., Rugh, M.B., Feraud, M., Hung, W.-.C., Jay, J., Cao, Y., Parker, E.A., Grant, S.B., Holden, P.A, 2021. Limited bacterial removal in full-scale stormwater biofilters as evidenced by community sequencing analysis. Environ. Sci. Technol. 55 (13), 9199–9208.
- Lotse, E.G., Jabro, J.D., Simmon, K.E., Baker, D.E, 1992. Simulation of nitrogen dynamics and leaching from arable soils. J. Contam. Hydrol. 10, 183–196.
- McPhillips, L., Walter, M.T., 2015. Hydrologic conditions drive denitrification and greenhouse gas emissions in stormwater detention basins. Ecol. Eng. 85, 67–75.
- McPhillips, L., Goodale, C., Walter, M.T., 2018. Nutrient leaching and greenhouse gas emissions in grassed detention and bioretention stormwater basins. J. Sustain. 4 (1), 04017014
- Morse, N.R., McPhillips, L.E., Shapleigh, J.P., Walter, M.T., 2017. The role of denitrification in stormwater detention basin treatment of nitrogen. Environ. Sci. Technol. 51 (14), 7928–7935.
- Morse, N., Payne, E., Henry, R., Hatt, B., Chandrasena, G., Shapleigh, J., Cook, P., Coutts, S., Hathaway, J., Walter, M.T., McCarthy, D, 2018. Plant-microbe interactions drive denitrification rates, dissolved nitrogen removal, and the abundance of denitrification genes in stormwater control measures. Environ. Sci. Technol. 52 (16), 9320–9329.
- National Oceanographic and Atmospheric Administration (2021). California Nevada River Forecast Center: Observed Precipitation.
- Parker, E.A., Grant, S.B., Cao, Y., Rippy, M.A., McGuire, K.J., Holden, P.A., Feraud, M., Avasarala, S., Liu, H., Hung, W.C., Rugh, M., Jay, J., Peng, J., Shao, S., Li, D, 2021. Predicting solute transport through green stormwater infrastructure with unsteady transit time distribution theory. Water Resour. Res. 57, e2020WR028579.
- Parker, E.A., Grant, S.B., Sahin, A., Vrugt, J.A., Brand, M.W., 2022. Can smart stormwater systems outsmart the weather? Stormwater capture with real-time control in Southern California. ACS ES&T Water 2 (1), 10–21.
- Parkin, T.B., 1987. Soil microsites as a source of denitrification variability. Soil Sci. Soc. Am. J. 51, 1194–1199.
- Payne, E.G., Fletcher, T.D., Cook, P.L., Deletic, A., Hatt, B.E., 2014a. Processes and drivers of nitrogen removal in stormwater biofiltration. Crit. Rev. Environ. Sci. Technol. 44 (7), 796–846.

- Payne, E.G., Fletcher, T.D., Russell, D.G., Grace, M.R., Cavagnaro, T.R., Evrard, V., Deletić, A., Hatt, B.E., Cook, P.L., 2014b. Temporary storage or permanent removal? The division of nitrogen between biotic assimilation and denitrification in stormwater biofiltration systems. PLoS ONE 9, e90890.
- Philippot, L., Hallin, S., Schloter, M., 2007. Ecology of denitrifying prokaryotes in agricultural soil. Adv. Agron. 96, 249–305.
- Read, J., Fletcher, T.D., Wevill, T., Deletic, A., 2010. Plant traits that enhance pollutant removal from stormwater in biofiltration systems. Int. J. Phytoremediation 12, 34–53.
- Rugh, M.B., Grant, S.B., Hung, W.C., Jay, J.A., Parker, E.A., Feraud, M., Li, D., Avasarala, S., Holden, P.A., Liu, H., Rippy, M.A., 2022. Highly variable removal of pathogens, antibiotic resistance genes, conventional fecal indicators and humanassociated fecal source markers in a pilot-scale stormwater biofilter operated under realistic stormflow conditions. Water Res. 219, 118525.
- Sage, J., Berthier, E., Gromaire, M.C., 2015. Stormwater management criteria for on-site pollution control: a comparative assessment of international practices. Environ. Manag. 56 (1), 66–80.
- Schlesinger, W.H., 2009. On the fate of anthropogenic nitrogen. Proc. Natl Acad. Sci. 106, 203–208.
- Sigman, D.M., Granger, J., DiFiore, P.J., Lehmann, M.M., Ho, R., Cane, G., van Geen, A., 2005. Coupled nitrogen and oxygen isotope measurements of nitrate along the eastern North Pacific margin. Global Biogeochem. Cycles 19 (4), GB4022.
- Spoelstra, J., Schiff, S.L., Hazlett, P.W., Jeffries, D.S., Semkin, R.G., 2007. The isotopic composition of nitrate produced from nitrification in a hardwood forest floor. Geochim. Cosmochim. Acta 71, 3757–3771.
- Steffen, W., Richardson, K., Rockström, J., Cornell, S.E., Fetzer, I., Bennett, E.M., Biggs, R., Carpenter, S.R., De Vries, W., De Wit, C.A., Folke, C., 2015. Planetary boundaries: Guiding human development on a changing planet. Science 347 (6223), 1259855
- U.S. EPA. (1993). Method 353.2: Determination of Nitrate-Nitrite Nitrogen By Automated Colorimetry. Revision 2.0. Cincinnati, OH.
- U.S. EPA. (1993). Method 350.1: Nitrogen, Ammonia (colorimetric, Automated phenate), Revision 2.0. Cincinnati, OH.
- U.S. EPA. (1997). Method 300.1: Determination of Inorganic Anions in Drinking Water By Ion chromatography. Revision 1.0. Cincinnati, OH.
- Valenca, R., Le, H., Zu, Y.Y., Dittrich, T.M., Tsang, D.C.W., Datta, R., Sarkar, D., Mohanty, S.K., 2021. Nitrate removal uncertainty in stormwater control measures: is the design or climate a culprit? Water Res. 190, 116781.
- Waller, L.J., Evanylo, G.K., Krometis, L.A.H., Strickland, M.S., Wynn-Thompson, T., Badgley, B.D., 2018. Engineered and environmental controls of microbial denitrification in established bioretention cells. Environ. Sci. Technol. 52 (9), 5358–5366.
- Walsh, C.J., Leonard, A.W., Ladson, A.R., and Fletcher, T.D. (2004). Urban Stormwater and the Ecology of streams. Cooperative Research Centre for Freshwater Ecology and Cooperative Research Centre for Catchment Hydrology, Canberra, Australia.
- Wang, L., Xin, J., Nai, H., Zheng, T., Tian, F., Zheng, X., 2020. Sorption of DONs onto clay minerals in single-solute and multi-solute systems: implications for DONs mobility in the vadose zone and leachability into groundwater. Sci. Total Environ. 712, 135502.
- Zinger, Y., Blecken, G.T., Fletcher, T.D., Viklander, M., Deletić, A., 2013. Optimising nitrogen removal in existing stormwater biofilters: benefits and tradeoffs of a retrofitted saturated zone. Ecol. Eng. 51, 75–82.